Article

Ag Nanoparticles-Based Zinc Hydroxide-Layered Hybrids as Novel and Efficient Catalysts for Reduction of 4-Nitrophenol to 4-Aminophenol

Fernando Junior Quites,[*,a] *Camila K. S. Azevedo,*[a] *Everton P. P. Alves,*[a]
José Carlos Germino,[b] *Rita C. G. Vinhas,*[c] *Richard Landers,*[c] *Ailton José Terezo*[a] *and*
Teresa D. Z. Atvars[b]

[a]*Departamento de Química, Instituto de Ciências Exatas e da Terra, Universidade Federal de Mato Grosso (UFMT), 78060-900 Cuiabá-MT, Brazil*

[b]*Instituto de Química and* [c]*Departamento de Física Aplicada, Instituto de Física Gleb Wataghin, Universidade Estadual de Campinas (UNICAMP), 13083-970 Campinas-SP, Brazil*

Silver nanoparticles and zinc hydroxide-layered hybrid materials (AgNPs/ZHL) have been successfully developed as efficient catalysts for the reduction of 4-nitrophenol (4-NP) to 4-aminophenol (4-AP) with sodium borohydride. A facile and rapid visible-light assisted green route was used for the deposition of silver nanoparticles (AgNPs) on the external surface of ZHL material. The resulting AgNPs/ZHL hybrids contained AgNPs with spherical morphology and uniform size distribution. Moreover, the AgNPs/ZHL compounds exhibited excellent catalytic performance (the reduction reaction was finished within 4 min) and reusability (three cycles) toward the reduction of 4-NP to 4-AP in presence of sodium borohydride. The reduction reaction obeyed the pseudo-first-order kinetics. The rate constants increased with the increase of amount of the AgNPs deposited into the hybrid materials. These results suggest that the as-prepared catalysts (AgNPs/ZHL) have great potential for heterogeneous catalytic applications.

Keywords: Ag nanoparticles, layered material, catalysis, 4-nitrophenol

Introduction

Nitrophenolic compounds and their derivatives are environmental pollutants which sources may be as different as industrial effluents or the reaction products and degradation of certain pesticides, dyes, etc.[1-3] Therefore, reduction reaction of 4-nitrophenol (4-NP) to 4-aminophenol (4-AP) is important because nitrophenols and their derivatives are obtained during the production of herbicides, pesticides, synthetic dyes, etc.[1,2] Thus, a great deal of efforts have been challenged on the reduction of 4-NP to 4-AP in the last years.[1-3] Among them, the borohydride reduction of 4-NP to 4-AP by metal nanoparticles such as Ag, Au, Pt and Cu is particularly attractive because this reaction can be performed in aqueous solution under mild condition.[1-10]

Metal nanoparticles (NPs) have a variety of interesting properties, which enable them to play significant roles in a broad range of optic-electronic, biochemical and catalytic applications.[1,3,4] In special, silver nanoparticles (AgNPs) have become a central topic of academic and industrial interest as a promising candidate for next-generation nanocatalysts.[5] AgNPs were the first one of metal nanocatalysts to be employed for the reduction of 4-NP to 4-AP in presence of NaBH$_4$.[6] However, metal NPs are generally unstable due to their large active surface areas, so preventing their self-aggregation, which causes a huge drop in a catalytic activity, is critical for practical use. Surface coating with surfactants and/or various chemical modifications of the metal NPs have been carried out to stabilize them and maintain the original size dispersions.[2,3,7] Another effective approach to inhibit aggregation is to immobilize the metal NPs onto the various supports, such as metal oxides,[1,2,8] boron nitride[4] or layered materials.[9] In fact, layered material-NPs hybrids are attracting attention for practical applications due to their mechanical and catalytic properties.[1,9,11] AgNPs have been deposited in different inorganic substrates for use as catalysts in reduction of 4-NP to 4-AP with NaBH$_4$ in excess. Recently, Hsu and Chen[10] showed a rapid microwave-assisted green route for the uniform deposition of Ag nanoparticles on graphene oxide surface with L-arginine acting as the external reducing

*e-mail: fquitesquim@gmail.com, fquites@ufmt.br

agent. Zhang *et al.*[11] investigated also the catalytic properties of hybrids based on silica nanowires and AgNPs using *in situ* reduction of Ag^{+} ions by NaBH$_4$ on silica nanowires. According to the studies performed by these authors, AgNPs/silica hybrids exhibited high catalytic activities because the nearly monodispersed AgNPs were embedded on the surface of SiO$_2$ nanowires, allowing active contact between the reactants (4-NP and NaBH$_4$) and catalyst of the reaction.

Layered compounds have been widely used as supporting material in catalyst systems due to their chemical stabilities and thermal properties.[9,12,13] In this type of materials, the guest species may be adsorbed both on the external surfaces and/or into the interlayer spacing. In this sense, layered hydroxide salts (LHS) are interesting materials as hosts in intercalation/adsorption reactions.[9,12,14] LHS have a double layered hydroxides (HDS) structure which is similar to that of brucite;[12-14] however, the inorganic layers are composed of only one type of metal cation such as Cu^{2+}, Zn^{2+} and Ni^{2+} and can be represented by the general formula, $M^{2+}(OH)_{2-x}(A^{n-})_{x/n} \cdot yH_2O$.[12-14] In this structure, the hydroxyl anions on the brucite hydroxide layer are substituted by water molecules and counter anions.[12-14] A[n-] is the exchangeable anion and y represents the water content of the interlayer region. When the metal cation (M[2+]) in this structure are Zn^{2+} ions and the A[n-] counter ions are nitrate anions, it is known as zinc hydroxide-layered in nitrate form (ZHL) belonging to the LHS family.[13,14] The structure of the aforementioned ZHL, $Zn_5(OH)_8(NO_3)^{2-} \cdot 2H_2O$, can be considered a structural variation of the Zn(OH)$_2$ structure, where one fourth of the octahedral Zn^{2+} cations are removed from the layer.[12,13] Every octahedral site occupied by a Zn^{2+} cation shares edges with two empty and four occupied octahedra, producing a layer with a residual negative charge ($[Zn_3(OH)_8]^{2-}$).[12] To compensate for the deficit in positive charge, tetrahedral Zn^{2+} cations accommodate below and above the empty octahedra of the layer. In this way, three corners of the tetrahedra coordinate with oxygen atoms of the layer, whereas the fourth position coordinates with a water molecule. In this configuration, the layer is positively charged $[Zn_{3(oct.)}(OH)_8Zn_{2(tet.)}(H_2O)_2]^{2+}$, where oct. and tet. represent the Zn^{2+} cations located in octahedral and tetrahedral sites, respectively.[12] To neutralize the residual positive charge of the layer, anions intercalate between the layers. Nitrate anions intercalate between the layers in the case discussed here.[12-14] ZHL material can be easily employed as support for the intercalation reaction of the different anionic guests.[13,14] Recently, we used this inorganic layered compound as host for the intercalation of luminescent anionic pyranine organic dye.[14]

Inspired by the above-mentioned considerations, in this study, we demonstrated the green synthesis of AgNPs-dispersed on ZHL support. Initially, different amounts of Ag^{+} ions were adsorbed on the external surfaces of ZHL followed by their rapid reduction by visible-light, at room temperature, using one-pot method.[15] Using this method, we have achieved the growth and stabilization of spherical shaped AgNPs on the external surfaces of zinc hydroxide-layered for the production of AgNPs/ZHL hybrids. Ag nanoparticles were chosen because they were cheaper as compared to other noble metal catalysts such as Au and Pt.[1,2,5,9,10] Finally, the catalytic activities of AgNPs/ZHL hybrids were investigated for the reduction of 4-nitrophenol to 4-aminophenol in presence of NaBH$_4$. These materials exhibited high catalytic activity and they could be easily reused several times. To the best of our knowledge, this is the first report using AgNPs/ZHL hybrid catalysts for reduction of 4-NP to 4-AP at room temperature.

Experimental

Materials

Zinc nitrate hexahydrate (Zn(NO$_3$)$_2$·6H$_2$O, reagent grade, 98%), sodium hydroxide (NaOH pellets) and 4-NP (99%) were purchased from Sigma-Aldrich (São Paulo, Brazil). Silver nitrate (AgNO$_3$) was supplied by Merck (São Paulo, Brazil). Reagents and solvents were of reagent grade and were used without further purification.

Zinc hydroxide-layered in nitrate form (ZHL) was synthesized according to the procedure described by Quites *et al.*[14]

Preparation of the AgNPs(x)/ZHL hybrids

AgNPs/ZHL materials were synthesized by a facile, rapid and green simple process. Firstly, 0.300 g of ZHL was dispersed in 50 mL of AgNO$_3$ ethyl alcohol solution with constant stirring at room temperature. After 1 h of further reaction, the dark brown product was collected by centrifugation, washed with distilled water and ethanol several times each, and finally, air-dried at room temperature. To investigate the effect of the content of Ag nanoparticles on ZHL two samples were prepared, under the same experimental conditions, AgNPs(1)/ZHL and AgNPs(2)/ZHL with different amounts of Ag^{+} ions: 0.038 and 0.065 mol L^{-1}, respectively.

Catalytic activity of AgNPs(x)/ZHL particles in reduction of 4-NP by NaBH$_4$

The catalytic activity of AgNPs(x)/ZHL hybrids in reduction of 4-NP by NaBH$_4$ was also investigated. For

the catalytic reduction of 4-NP, fresh $NaBH_4$ (0.5 mL, 0.88 mol L^{-1}) was mixed with an aqueous solution of 4-NP (25 mL, 1.50 mmol L^{-1}).[16] After the solution changed from light yellow to deep yellow, 10 mg of AgNPs(x)/ZHL catalyst was added. Since the UV absorbance of 4-NP is linearly proportional to its concentration in the solution, the ratio of the absorbance at time t (A_t) to that at t = 0 (A_0) is equal to the concentration ratio C_t/C_0 of 4-NP.[16] Consequently, the conversion progress can be directly measured using the absorption intensity. The progress of the conversion of 4-NP to 4-AP was monitored in a Varian Cary 50 spectrophotometer. The pseudo-first order kinetics model was used to describe the catalytic reaction progress.[1,2,16] The reaction rate, k, was calculated from the rate law by means of equation 1:

$$\ln \frac{A_t}{A_0} = -kt \qquad (1)$$

in which A_t is the absorbance at time t and A_0 is the initial absorbance. In the absence of any catalyst the reaction is not completed even after 2-3 days. However, the AgNPs(x)/ZHL materials synthesized herein significantly enhance the rate of the reduction reaction.

The turnover frequency (TOF)[17] is defined as the number of moles of 4-nitrophenol converted *per* mole of silver *per* time unit, based on the amount of product formed after 4 min of reaction. Stability and reusability studies were addressed through centrifugation of the AgNPs/ZHL samples after completion of the reaction. The deposited catalyst was washed several times with ethanol to remove all organic substances, and then dried at room temperature before use in consecutive runs.

Conversion (%) and TOF (h^{-1}) were calculated according to the following equations:

$$\text{Conversion (\%)} = \frac{[C_0] - [C_t]}{[C_0]} \times 100 \qquad (2)$$

where $[C_0]$ is the initial 4-nitrophenol concentration, $[C_t]$ is the concentration of 4-nitrophenol at time (t).

$$\text{Turnover number (TOF)} = \frac{\dfrac{[C_0 - C_t]}{[Ag]}}{t} \qquad (3)$$

where $[C_0]$ is the initial 4-aminophenol concentration (in moles), $[C_t]$ is the concentration of 4-nitrophenol at time (t); and [Ag] is the concentration of AgNPs (in moles) in the catalyst sample.[17] TOF was calculated based on the total amount of AgNPs.

Instrumentation

The crystalline structures of AgNPs/ZHL hybrids were characterized by powder X-ray diffraction (XRD) analysis on Shimadzu XRD7000 diffractometer equipped with a copper target and graphite monochromator with Cu Kα (λ = 1.54 Å). The 2θ angle was scanned at a rate of 1° min^{-1} from 1.5 to 50° at room temperature. The Debye-Scherrer equation

$$D = 0.9\lambda / (\beta\cos\theta) \qquad (4)$$

was employed to estimate the size of the crystalline domains from the (200) diffraction plane of ZHL layered and their hybrids. The definition of each term in the equation is as follows: λ is the wavelength of Cu Kα radiation (λ = 0.1541 nm), β is the full width at half maximum of the (200) diffraction plane, θ is the Bragg's diffraction and D is the average size of the crystalline domains. Diffuse-reflectance UV-Vis spectra were recorded with PerkinElmer Lambda spectrophotometer of powder samples, equipped with a 150 mm integration sphere, using barium sulfate ($BaSO_4$) powder as reference. The UV-Vis spectra were collected in the spectral range of 200-800 nm and analyzed with the Kubelka-Munk equation using software provided by PerkinElmer. Fourier transformed infrared spectra (FTIR) of the samples were obtained from 4.000 to 400 cm^{-1} at 4 cm^{-1} resolution on a Nicolet 6700 spectrometer in pellets of samples dispersed in KBr. The morphology and composition of the samples were determined by scanning electron microscopy (SEM) and by energy-dispersive X-ray spectroscopy (EDS-SEM) on a FEGLEO 1525 scanning electron microscope (FE-SEM). For the FE-SEM images, a small drop of the isopropanol dispersion was deposited on the sample holder and then evaporated in air at room temperature. The high-resolution transmission electron microscopy (HRTEM) images were obtained on a JEOL Model JEM-2100 F electron microscope with an accelerating voltage of 200 kV. For investigating the AgNPs structure in the hybrids, X-ray photoemission spectra (XPS) measurements were performed on a VSW HA100 spectrometer using non-monochromatized Kα of Al (1486.6 eV) radiation. The data were obtained at room temperature, and typically the operating pressure in the analysis chamber was below 2×10^{-8} mbar. The calibration of binding energies (BEs) was performed with Au $4f_{7/2}$ core level at 84.0 eV, and BE of adventitious carbon (284.6 eV) was utilized for charging correction with all the samples. The error in all the BE values reported here is within ± 0.3 eV.

Results and Discussions

Structural and morphologic characterization of AgNPs(x)/ZHL hybrids

The visual change of color suspension from white to yellowish brown by adding the ZHL support to the $AgNO_3$ ethanol solution was the first observation to the AgNPs/ZHL hybrids production. In this system, under visible-light,[15] the Ag^+ ions were reduced to Ag^0, where the metal silver nanoparticles were anchored on ZHL material (see images of experimental synthesis in Figure S1 in the Supplementary Information).

The XRD patterns of the starting material as well as of the AgNPs(x)/ZHL solids obtained after each step of the *in situ* reduction of Ag^+ ions under visible-light are given in Figure 1. The ZHL particles presented a layered structure with the sheets separated by a d-spacing of 0.98 nm, where the nitrate ions are occluded between the inorganic lamellae (Figure 1a).[11-14] This pattern is identified as zinc hydroxide nitrate layered (JCPDS card 24-1460) and it is characterized by an intense and sharp reflection at 0.98 nm (2θ = 9.05), due to the (200)-plane of the monoclinic structure.[11,14] All AgNPs(x)/ZHL hybrids (curves *ii* and *iii* in Figure 1a) exhibited the same diffraction peaks of pristine ZHL indicating that the AgNPs do not disturb the layered structure of inorganic support. In addition, the basal spacing of ZHL (d_{200} = 0.98 nm) did not change upon the reduction reaction with AgNPs, suggesting that they are localized on the external surfaces of the ZHL support. From the XRD patterns, the size of the crystalline domains of ZHL, AgNPs(1)/ZHL and AgNPs(2)/ZHL materials were calculated as 280, 385 and 446 nm, respectively. These results indicated that the size of crystalline domains of the ZHL layered is increased with increasing AgNPs content.

FTIR spectra for the hybrid materials also indicated that the AgNPs do not disturb the vibrations of ZHL host (see Figure S2 in Supplementary Information).

We have also studied the UV-Vis absorption spectra of AgNPs(x)/ZHL hybrid compounds as an optical tool for the characterization of AgNPs in the ZHL matrix. In all hybrids one broad surface plasmon resonance peak (SPR) in the range of 370-470 nm (maximum centered at 420 nm) was observed (Figure 1b, curves *ii* and *iii*), which is the characteristic of spherical Ag nanoparticles.[4,8,9,14] Moreover, the color of the AgNPs/ZHL hybrids is yellow-green, which is different to that of the pure ZHL compound (see the inset of Figure 1b). They are similar to those reported in the literature,[5,9,16] indicating the existence of AgNPs in AgNPs/ZHL hybrids. The content of Ag nanoparticles on the ZHL
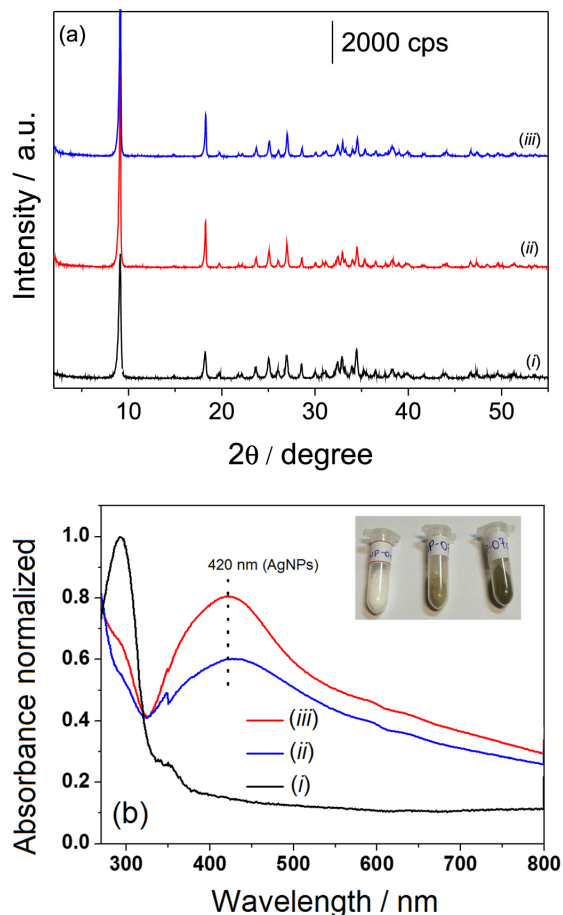

Figure 1. (a) XRD patterns and (b) UV-Vis reflectance diffuse spectra of (*i*) pure ZHL and of their hybrids (*ii*) AgNPs(1)/ZHL and (*iii*) AgNPs(2)/ZHL. Inset in Figure 1b shows the photograph image of ZHL and AgNPs(x)/ZHL materials.

host is about 0.7 and 1.8 wt.% for the AgNPs(1)/ZHL and AgNPs(2)/ZHL hybrids, respectively, investigated by X-ray photoemission (see below).

The morphology of the samples was also studied by SEM. ZHL support showed irregular sheets with thickness of several tens of nanometers, which were obtained by the chemical precipitation method (Figures 2a and 2b).[15] From SEM images of AgNPs(2)/ZHL hybrid (Figures 2c and 2d) is clearly seen that spherical AgNPs with mean diameters and standard deviation of 21 ± 12 nm were deposited on ZHL surfaces. Figures 2c and 2d also show that the AgNPs are almost uniformly anchored on both sides of the sheets. Furthermore, the morphology and size of the ZHL sheets in the hybrids did not change obviously compared to those of ZHL sheets, that is, the ZHL sheets are stable during formation of the hybrids, as also verified by the XRD and FTIR techniques. Typical HRTEM micrograph (see inset in Figure 2d) for the AgNPs(2)/ZHL hybrid clearly indicated the formation of uniformly distributed spherical Ag nanoparticles with distinct size distributions on the
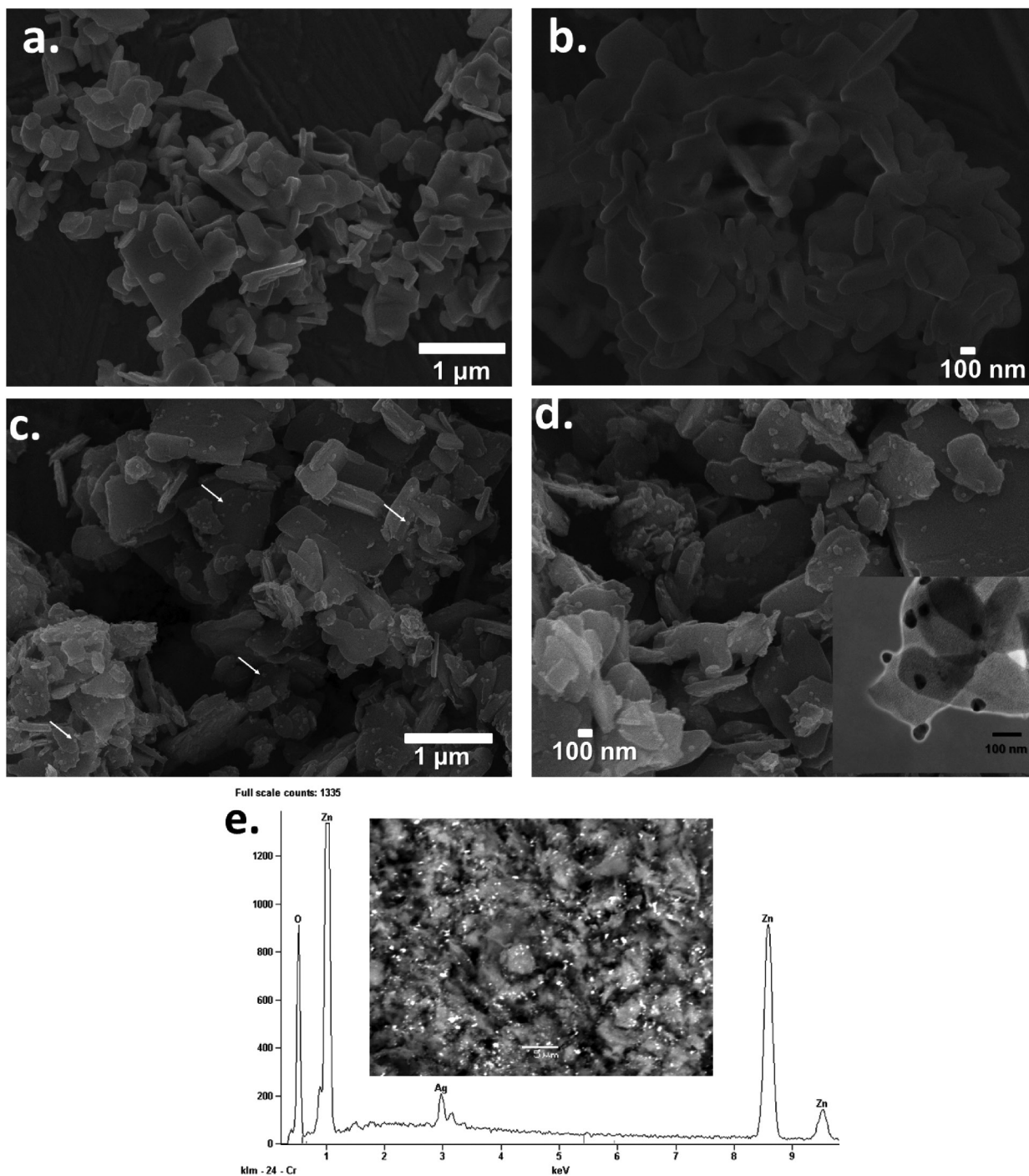
Figure 2. SEM images at (a) low (scale bar: 1 µm) and (b) high resolution (scale bar: 100 nm) of pure ZHL; SEM images at (c) low (scale bar: 1 µm) and (d) high resolution (scale bar: 100 nm) of AgNPs(2)/ZHL hybrids and (e) typical EDS-SEM spectrum of AgNPs(2)/ZHL particles. The arrows in Figure 2c indicate the presence of AgNPs on the surfaces of ZHL material. Inset in Figure 2d shows HRTEM image (scale bar: 100 nm).

ZHL surfaces, consistent with observations from the SEM images and UV-Vis spectroscopy. Additionally, an analysis of energy-dispersive X-ray spectroscopy (EDS-SEM) results (Figure 2e) indicated the presence of strong silver signal, which also confirm the presence of AgNPs, and absorption peaks of zinc and oxygen, which indicates that the AgNPs are deposited on ZHL inorganic support.

In order to further confirm the composition and structure of samples, XPS spectra were measured. XPS spectroscopy has been utilized as a useful tool for qualitatively determining the surface component and composition of the samples.[18-22] Figure 3a shows a survey scan in the range of 0-1000 eV. The peaks on the curve of the AgNPs(2)/ZHL hybrid sample are assigned to Zn, N, O, Ag, and C

elements. The C element was attributed to the adventitious carbon-based contaminant. Therefore, it is concluded that Ag exists in the hybrid materials, while Zn, N and O exist in all samples. In order to determine the chemical environment and oxidation state of silver atoms on the ZHL surface, we have performed XPS measurement of the Ag 3d core levels. Figure 3b exhibits the core level Ag 3d spectra of the AgNPs(2)/ZHL hybrid, showing two distinct individual peaks for Ag $3d_{5/2}$ and Ag $3d_{3/2}$ at 368.2 and 374.2 eV, respectively, with ca. 6 eV splitting between the two peaks, which is evidence of the reduction of Ag^+ ions assisted by under light-visible to produce metallic silver[10] in good agreement with bulk silver metallic values.[18,19] This is attributed to the complete reduction[18] of Ag^+ to Ag^0, further confirming that there is an interaction between the ZHL sheets and AgNPs. The Ag $3d_{5/2}$ peak for the AgNPs(1)/ZHL hybrid (Figure 3c) appears at a binding energy of 367.4 eV, and the splitting of the 3d doublet is 6.0 eV, indicating the metallic nature of the silver. For this hybrid material, interestingly, the $3d_{5/2}$ peak of Ag in our work was found to shift obviously to the lower binding energy compared with the standard value (about 368.2 eV for bulk Ag).[19,20,22] This confirms the interaction between Ag and ZHL support as the binding energy of monovalent Ag is known to be much lower than that of zerovalent Ag. Similar results were also found in Lin *et al.* work.[18] In the literature it has been reported that core levels shifts to lower binding energies for small Ag nanoparticles,[21,22] this can also influence the binding energy of Ag 3d for the AgNPs(1)/ZHL, which presented lower amount of AgNPs.

Based on the previously mentioned-characterization techniques, the as-prepared hybrids (AgNPs(x)/ZHL) presented a layer structure and not only have high adsorption capacity for the AgNPs, but also showed high visible-light absorption activity due to the presence of AgNPs. These results are in excellent agreement with the studies realized by Marcato *et al.*,[23] which deposited biogenic AgNPs on the external surfaces of LDH material employing fungi *Fusarium oxyporum* as external reducing agent for the Ag^+ ions. According to these authors, the high adsorption capacity of the AgNPs by the LDH material can be associated to the interactions between metal nanoparticles and layered material manifested from electrostatic interactions between the negatively charged AgNPs ($\zeta = -13.2$ mV) and positively charged layered compound ($\zeta = +3.2$ mV).[18]

In a previous work by our group,[9] we reported on a reproducible and simple approach to the synthesis of nanocomposites based on gold metal nanoparticles (AuNPs) and layered zinc hydroxide. ZHL was used as support for the deposition of the gold nanoparticles. It was demonstrated that gold nanoparticles were rapidly formed when ZHL layered was added to the ethanol chloroauric acid solution at room temperature and under visible-light. In this system, the ethyl alcohol acted as a solvent of the gold precursor and as a reducing agent, where the Au^{3+} ions were mainly reduced via redox reaction between the
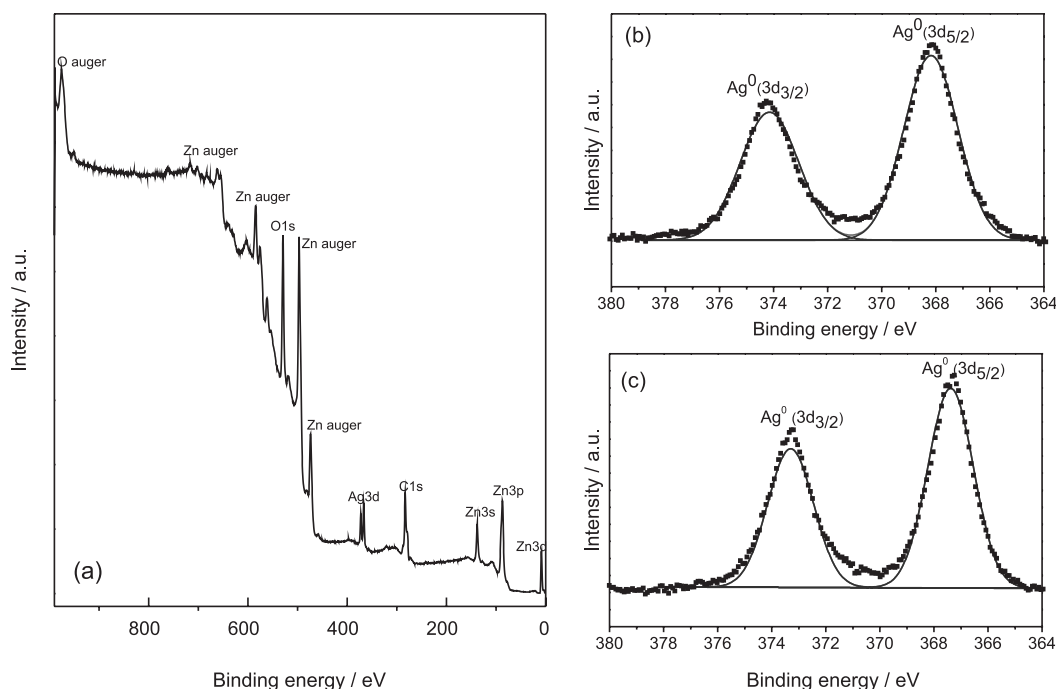

Figure 3. (a) XPS fully scanned spectra and XPS spectra of Ag 3d of the hybrids (b) AgNPs(2)/ZHL and (c) AgNPs(1)/ZHL.

metallic precursor and the solvent. Measurements from gas chromatography-mass spectrometry demonstrated that the AuNPs were produced with the formation of acetaldehyde. The AuNPs/ZHL nanocomposites were also used as templates for the production of the AuNPs/ZnO.[9] Based on these considerations, we can conclude that the similar process occur in the system here studied, where ethanol molecules are oxidized to the acetaldehyde and silver ions are reduced to the AgNPs on the ZHL surface.

Application of AgNPs(x)/ZHL hybrids as catalysts for reduction of 4-NP

To study the catalytic property of the synthesized AgNPs containing ZHL catalysts, we have investigated the reduction reaction of 4-nitrophenol to 4-aminophenol in the presence of sodium borohydride in excess. To establish energy saving and environmentally friendly process, room temperature and distilled water were chosen as the reaction conditions.[1,2,16] Before reaction, the original absorption peak of 4-NP was seen at 316 nm (Figure 4a). After addition of excess NaBH$_4$ solution, the color of the solution immediately changed from pale yellow to yellow; meanwhile, a new absorption band appeared at 400 nm, which was attributed to the formation of 4-nitrophenolate ion in the alkaline medium caused by NaBH$_4$ (Figure 4a).[1,16] Without adding catalyst, the reduction is very slow, and the maximum absorption peak remained unaltered until 2 h of experimental observation. After AgNPs(x)/ZHL hybrids were added, the intensity of absorption band at 400 nm decreased, and at the same time, a new absorption band for 4-AP appeared at 298 nm (Figures 4a and 4b). After the reduction of 4-nitrophenol, the band at 400 nm was completely disappeared and the UV band at 298 nm, related to the 4-AP absorption, was increased. The reaction was finished within 6 min after being catalyzed with AgNPs(1)/ZHL and 4 min for AgNPs(2)/ZHL material (Figures 4a and 4b). No reaction occurred when we performed the reaction in the presence of pure ZHL and in the absence of catalyst (see Figure S3 in the Supplementary Information). This confirmed that the catalytic ability of AgNPs for the reduction of 4-NP to 4-AP resulted from silver nanoparticles deposited on ZHL support.

The concentration of NaBH$_4$ is so high compared with that of 4-NP that the reaction can be assumed to follow pseudo-first order reaction kinetics.[15,16] In Figure 5, a good linear correlation between the plot of ln (A$_t$/A$_0$) and reaction time was observed in the presence of the hybrid catalysts. The rate constant (k) calculated from the slope of the plot was 0.394 min^{-1} for AgNPs(1)/ZHL and 0.875 min^{-1} for AgNPs(2)/ZHL, which is comparable to that of other AgNPs deposited on inorganic substrate for 4-NP

reduction.[16,24,25] The rate of the catalytic reaction was higher in the case of AgNPs(2)/ZHL, which can be associated to the higher amount of AgNPs (Table 1). As observed by Naik *et al.*,[26] the rate of catalytic reaction is affected by the concentration or loading level of the catalytically active site (here in this work due to the presence of AgNPs).
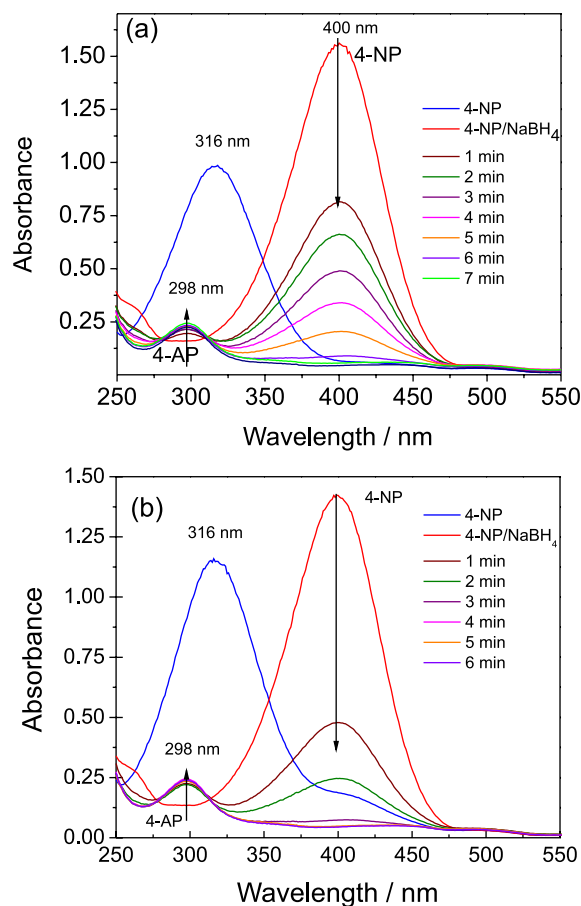

Figure 4. UV-Vis absorption spectra of 4-NP (blue curve) following the adding of NaBH$_4$ solution, but without the addition of catalysts (red curve), and others displayed the time-dependent, measured at 1 min intervals, of 4-NP reduction to 4-AP by (a) AgNPs(1)/ZHL and (b) AgNPs(2)/ZHL materials.

Table 1. Pseudo-first-order kinetics study of 4-NP reduction over different AgNPs/ZHL hybrid catalysts

Catalyst	k / min^{-1}	R^2	Conversion[a] / %	TOF[a] / h^{-1}
AgNPs(1)/ZHL	0.394 ± 0.011	0.9940	80	38.9
AgNPs(2)/ZHL	0.875 ± 0.052	0.9859	100	40.8

[a]Measured at 4 min time reaction. TOF: turnover frequency.

A comparison between the catalytic behaviors of different AgNPs supported on inorganic materials based on the rate constant k calculation of each catalyst was done (Table 2). For example, Chi *et al.*[27] reported the reduction of

4-NP to 4-AP over AgNPs-decorated $Fe_3O_4@SiO_2$ magnetic nanocomposite, k of 1.27×10^{-4} min^{-1} was obtained with a silver loading of 8.89%. In another study, Dang *et al.*[28] demonstrated the reduction of 4-NP over AgNPs on polymer particles with dendrimer@SiO$_2$, the k calculated was 0.305 min^{-1}. Zhang *et al.*[29] studied the synthesis of Fe_3O_4/P(MBAAm-*co*-MAA) nanochains as stabilizers for Ag nanoparticles and templates for hollow mesoporous structure. These authors obtained k of 0.342 min^{-1}. Evolution of AgNPs within an aqueous dispersion of nanosized zeolite Y was investigated by Severance and Dutta.[30] In this system, k for 4-NP reduction was 2.83×10^{-3} min^{-1}. Zhang *et al.*[11] demonstrated the reduction of 4-NP over AgNPs on chrysotile support, the k calculated was 0.4×10^{-4} min^{-1}. Li *et al.*[31] demonstrated a facile solid-state synthesis of Ag/graphene oxide nanocomposites as highly active and stable catalyst for the reduction of 4-nitrophenol with k of 0.493 min^{-1}. From these studies, it is clear that the catalytic performance of AgNPs(2)/ZHL hybrid (see TOF in Table 1) was superior to other Ag-containing inorganic (e.g., iron oxide, silica or graphene oxide) hybrid materials (Table 2).[10,26-31] This can be attributed to the deposition of AgNPs on external surfaces of ZHL, which gives high accessibility of the substrates to the active sites. In addition to the higher activity of AgNPs/ZHL catalysts, the one-pot synthetic procedure is also an advantage, surface modification was not needed, and light-visible irradiation was used as a reducing agent of Ag$^+$ ions. These results clearly suggest that ZHL acts as an excellent supporting material for Ag nanocatalysts. High TOF values obtained in this paper (Table 1) are according to recently published research.[32-34]

Table 2. Comparison of reaction rates (k) for 4-nitrophenol reduction with different reported catalyst systems

Composition	k / min^{-1}	Reference
AgNPs/Fe$_2$O$_3$@SiO$_2$	1.27×10^{-4}	27
AgNPs/zeolite Y	2.83×10^{-3}	30
AgNPs/chrysotile	0.42×10^{-4}	11
AgNPs/SiO$_2$@dendrimer	0.305	28
AgNPs/Fe$_3$O$_4$	0.342	29
AgNPs/graphene oxide	0.493	31
AgNPs(1)/ZHL	0.394	this study
AgNPs(2)/ZHL	0.875	this study

Figure 6 exhibits the reusability of the AgNPs/ZHL hybrids for the catalytic reduction of 4-NP with NaBH$_4$ at room temperature. It was observed that 84 and 68% of catalytic activity was retained after reuse two and three times, respectively, revealing the good stability of catalyst. The reaction rates were 0.875 ± 0.052, 0.4733 ± 0.046
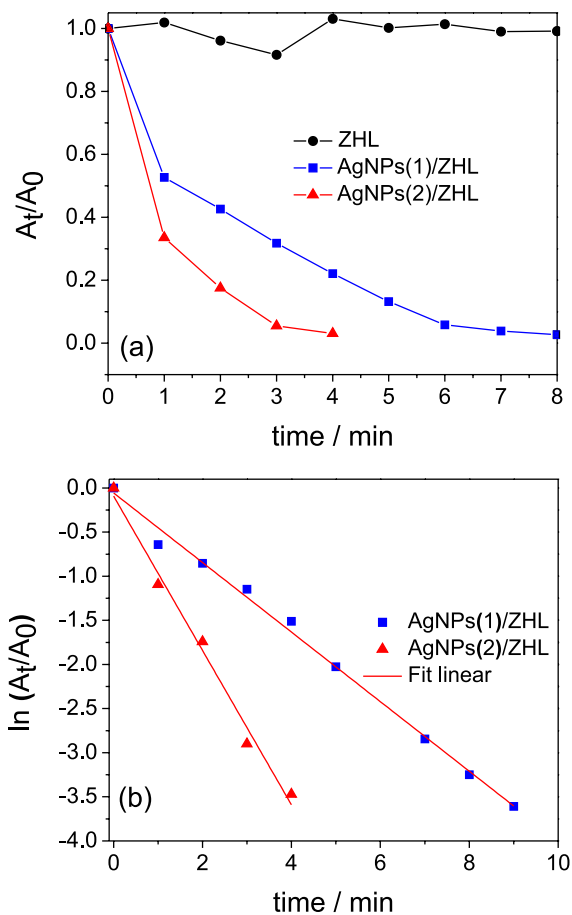

Figure 5. (a) Plot of (A$_t$/A$_0$) *versus* reaction time for the reduction of 4-nitrophenol by ZHL (full circle curve), AgNPs(1)/ZHL (full square curve) and AgNPs(2)/ZHL (full triangle curve) materials and (b) plot of ln (A$_t$/A$_0$) *versus* reaction time for the reduction of 4-nitrophenol by AgNPs(1)/ZHL (full square curve) and AgNPs(2)/ZHL (full triangle curve) materials at room temperature.
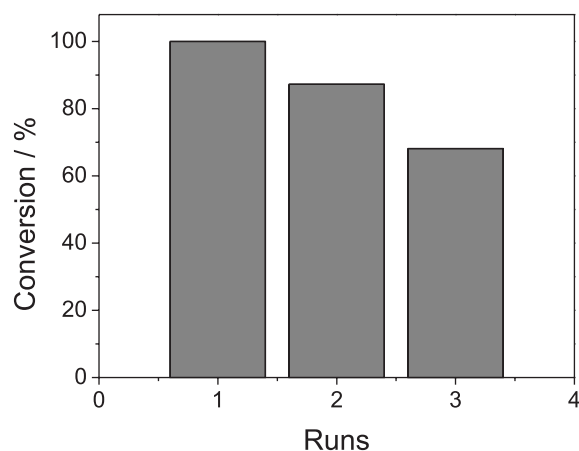

Figure 6. Reusability/stability test of AgNPs(2)/ZHL hybrid for the catalytic reduction of 4-NP with NaBH$_4$ at room temperature.

and 0.2574 ± 0.012 min^{-1} for the first, second and third cycles, respectively. This showed that the catalyst was not deactivated or poisoned significantly. The decrease of

catalytic activity might be due to the loss of the AgNPs/ZHL catalyst during the washing/centrifugation process because quite low catalyst concentration was used as well as the oxidation of the surface of the nanoparticles in the alkali solution.[10,31,35]

Based on all above considerations, we can claim that the AgNPs(x)/ZHL catalysts prepared in this work have good catalytic activity, consequently encourage the use of these materials as effective catalysts for the reduction of nitro-compounds. More importantly, no significant activity loss for the AgNPs/ZHL catalysts was observed after reuse for different cycles.

Conclusions

In summary, this report describes a facile and green approach to fabricate AgNPs/ZHL hybrids. Visible-light was used as reduction agent to produce AgNPs on the external surfaces of ZHL support. Compared with previous reports,[15-21] this fabrication process was carried in ethanol, without additional reductants or special equipment, which makes it less costly and eco-friendly. The SEM, XRD, and EDS-SEM analyses, the spectroscopic techniques (UV-Visible, FTIR and XPS) and visual observations showed the formation of AgNPs/ZHL hybrids. More importantly, AgNPs/ZHL hybrids showed excellent catalytic activity for the reduction of 4-NP to 4-AP with $NaBH_4$. In addition, the catalytic activity depended of AgNPs content on ZHL support, increasing the amount of AgNPs the time reduction of 4-NP to 4-AP is decreased. Reduction reactions catalyzed by AgNPs/ZHL were repeated in triplicate and reproducible results were obtained. The simplicity of this synthetic green route makes the as-prepared hybrids promising components in heterogeneous catalysis systems. Furthermore, the AgNPs-based hybrid system may find promising applications in other fields such as antibacterial studies. Works on these studies are in progress.

Supplementary Information

Supplementary data (photographic images showing the progress reaction at different times, FTIR spectra of hybrid materials and UV-Vis absorption spectra of 4-NP reduction in $NaBH_4$ presence by ZHL supporting material at room temperature) are available free of charge at http://jbcs.sbq.org.br as PDF file.

Acknowledgments

References

1. Xia, J.; He, G.; Zhang, L.; Sun, X.; Wang, X.; *Appl. Catal., B* **2016**, *180*, 408.

2. Zhao, P.; Feng, X.; Huang, D.; Yang, G.; Astruc, D.; *Coord. Chem. Rev.* **2015**, *287*, 114.

3. Hajfathalian, M.; Gilroy, K. D.; Yaghoubzade, A.; Sundar, A.; Tan, T.; Hughes, R. A.; Neretina, S.; *J. Phys. Chem. C* **2015**, *119*, 17308.

4. Shen, H.; Duan, C.; Guo, J.; Zhao, N.; Xu, J.; *J. Mater. Chem. A* **2015**, *3*, 16663.

5. Dong, X.-Y.; Gao, Z.-W.; Yang, K.-F.; Zhang, W.-Q.; Xu, L.-W.; *Catal. Sci. Technol.* **2015**, *5*, 2554.

6. Pradhan, N.; Pal, A.; Pal, T.; *Colloids Surf., A* **2002**, *196*, 247.

7. Azetsu, A.; Koga, H.; Isogai, A.; Kitaoka, T.; *Catalysts* **2011**, *1*, 83.

8. Li, Y.; Cao, Y.; Xie, J.; Jia, D.; Qin, H.; Liang, Z.; *Catal. Commun.* **2015**, *58*, 21.

9. Massola, B. C. P.; Souza, N. M. P.; Stachack, F. F. F.; Oliveira, E. W. R. S.; Germino, J. C.; Terezo, A. J.; Quites, F. J.; *Mater. Chem. Phys.* **2015**, *167*, 152.

10. Hsu, K.-C.; Chen, D.-H.; *Nanoscale Res. Lett.* **2014**, *9*, 484.

11. Zhang, H.; Duan, T.; Zhu, W.; Yao, W.-T.; J. Phys. Chem. C **2015**, 119, 21465.

12. Nakagaki, S.; Mantovani, K. M.; Machado, G. S.; Castro, K. A. D. F.; Wypych, F.; *Molecules* **2016**, *21*, 291.

13. Tavares, S. R.; Vaiss, V. S.; Wypych, F.; Leitão, A. A.; *Appl. Clay Sci.* **2015**, *114*, 103.

14. Quites, F. J.; Germino, J. C.; Atvars, T. D. Z.; *Colloids Surf., A* **2014**, *459*, 194.

15. Fan, H.; Zhu, J.; Sun, J.; Zhang, S.; Ai, S.; *Chem. Eur. J.* **2013**, *19*, 2523.

16. Tang, M.; Huang, G.; Li, X.; Pang, X.; Qiu, H.; *Mater. Chem. Phys.* **2015**, *162*, 31.

17. Hamdy, M. S.; *Microporous Mesoporous Mater.* **2016**, *220*, 81.

18. Lin, D.; Wu, H.; Zhang, R.; Pan, W.; *Chem. Mater.* **2009**, *21*, 3479.

19. Zhou, J.; Duan, X.; Ye, L.; Zheng, J.; Li, M. M. J.; Edman Tsang, S. C.; Yuan, Y.; *Appl. Catal., A* **2015**, *505*, 344.

20. Ma, L.; Wang, D.; Li, J.; Bai, B.; Fu, L.; Li, Y.; *Appl. Catal., B* **2014**, *148-149*, 36.

21. Prieto, P.; Nistor, V.; Nouneh, K.; Oyama, M.; Abd-Lefdil, M.; Díaz, R.; *Appl. Surf. Sci.* **2012**, *258*, 8807.

22. Gatemala, H.; Pienpinijtham, P.; Thammacharoen, C.; Ekgasit, S.; *CrystEngComm* **2015**, *17*, 5530.

23. Marcato, P. D.; Parizotto, N. V.; Martinez, D. S. T.; Paula, A. J.; Ferreira, I. R.; Melo, P. S.; Durán, N.; Alves, O. L.; *J. Braz. Chem. Soc.* **2013**, *24*, 266.

24. Mao, Y.; Wei, J.; Wang, C.; Feng, Y.; Yang, H.; Meng, X.; *Mater. Lett.* **2015**, *154*, 47.

25. Wang, Z.-Z.; Zhai, S.-R.; Zhai, B.; An, Q.-D.; Li, S.-W.; *J. Sol-Gel Sci. Technol.* **2015**, *75*, 680.

26. Naik, B.; Hazra, S. T.; Prasad, V. S.; Ghosh, N. N.; *Catal. Commun.* **2011**, *12*, 1104.

27. Chi, Y.; Yuan, Q.; Li, Y.; Tu, J.; Zhao, L.; Li, N.; Li, X.; *J. Colloid Interface Sci.* **2012**, *383*, 96.

28. Dang, G.; Shi, Y.; Fu, Z.; Yang, W.; *J. Colloid Interface Sci.* **2012**, *369*, 170.

29. Zhang, W.; Si, X.; Liu, B.; Bian, G.; Qi, Y.; Yang, X.; Li, C.; *J. Colloid Interface Sci.* **2015**, *456*, 145.

30. Severance, M.; Dutta, P. K.; *J. Phys. Chem. C* **2014**, *118*, 28580.

31. Li, Y.; Cao, Y.; Xie, J.; Jia, D.; Qin, H.; Liang, Z.; *Catal. Commun.* **2015**, *58*, 21.

32. Wang, M.; Fu, J.; Huang, D.; Zhang, C.; Xu, Q.; *Nanoscale* **2013**, *5*, 7913.

33. Chiou, J. R.; Lai, B. H.; Hsu, K. C.; Chen, D. H.; *J. Hazard. Mater.* 2013, *248*, 394.

34. Liu, X.; Jin, R.; Chen, D.; Chen, L.; Xing, S.; Xing, H.; Xing, Y.; Su, Z.; *J. Mater. Chem. A* **2015**, *3*, 4307.

35. Wu, C.-C.; Chen, D.-H.; *Nanoscale Res. Lett.* **2012**, *7*, 317.